



Wideband tunable Gaussian-shaped spectral filters based on dispersion engineering

Kuei-Chu Hsu^{a,*}, Nan-Kuang Chen^{b,c}, Sen-Yih Chou^{d,e}, Shien-Kuei Liaw^f, Yinchieh Lai^d, Sien Chi^{d,g}

^a Graduate Institute of Electro-Optical Engineering, Chang Gung University, Tao-Yuan 333, Taiwan, ROC

^b Department of Electro-Optical Engineering, National United University, Miaoli 360, Taiwan, ROC

^c Optoelectronics Research Center, National United University, Miaoli 360, Taiwan, ROC

^d Department of Photonics & Institute of Electro-Optical Engineering, National Chiao Tung University, Hsinchu 300, Taiwan, ROC

^e Center for Measurement Standards, Industrial Technology Research Institute, Hsinchu 300, Taiwan, ROC

^f Graduate Institute of Electro-Optical Engineering, National Taiwan University of Science and Technology, Taipei 106, Taiwan, ROC

^g Department of Electrical Engineering, Yuan Ze University, Chungli 320, Taiwan, ROC

ARTICLE INFO

Article history:

Received 21 September 2008

Revised 13 January 2009

Available online 26 April 2009

Keywords:

Gaussian filter

OCT

Fused-tapered

Efficiency

Thermo-optic

Dispersion engineering

ABSTRACT

Optical liquids can be used to engineer the dispersion characteristics of fibers by serving as the core or cladding to attain fundamental-mode cutoff effect. The short-/long-pass fiber filters are so made and concatenated to achieve widely thermo-optic tunable Gaussian-shaped spectral filters. The proposed wideband tunable Gaussian-shaped spectral filter provides a potential technique in application to high resolution bio-imaging.

© 2009 Elsevier Inc. All rights reserved.

1. Introduction

Broadband light sources with high spectral power density are important for high resolution optical coherence tomography (OCT) in cellular or tissue bio-imaging [1–3]. The broadband light source with a smooth Gaussian power spectrum is advantageous to achieve low speckle noise, generating from the mutually coherent scattering photons from biological tissues. Echo free OCT imaging can be obtained since a non-Gaussian-spectrum light source will significantly distort the OCT axial point spread function [4,5]. For non-Gaussian-spectrum light sources, the spectral modulation can cause echoes entering the axial point spread function, and the non-exponentially decay tails can cause the blindness of the weak reflection signals [5] to degrade the imaging. A Gaussian filter is usually required to shape the broadband light source into a Gaussian-spectral profile and to stabilize the output wavelengths. Gaussian-spectral filters are also widely used in various areas besides broadband light source imaging applications. For example, these filters are employed in the fiber laser cavity to shape the spectral profile of the laser output lights or in the optical communication systems to stabilize the system operation [6–8]. So far, the proposed Gaussian filters were made of a linear temperature gradient chirped fiber Bragg grating [9] or a large mode area photonic

crystal fiber (PCF) filled with high index liquid crystal (LC) in the holey cladding [10]. However, the typical passband bandwidth of the fiber Bragg grating may be too narrow to be used for the practical OCT systems and for the PCF fibers, the tuning efficiency is not very high due to the low temperature gradient of LC. The use of LC would also introduce extra birefringence for the guiding lights. Moreover, the Gaussian-shaped spectrum can only be obtained at certain fixed temperatures of LC and the bandwidth is not tunable.

In this work, we propose a new type of widely tunable Gaussian-shaped spectral filters by concatenating a short-wavelength-pass filter (SWPF) [11] and a long-wavelength-pass filter (LWPF) [12] based on our previous research results. The falling (rising) spectral curve of the SWPF (LWPF) is dispersion-engineered to fit the right (left) wing of the Gaussian profile through carefully adjusting the material and waveguide dispersions. For SWPF, the refractive index dispersion (RID) discrepancy between the optical liquid and silica tapered fiber is so large that the total internal reflection (TIR) criteria can only be satisfied at the wavelengths shorter than the cutoff point and the widely tunable short-pass filters are achieved accordingly. The tuning range is at least wider than 400 nm (1250–1650 nm) with a tuning efficiency higher than 50 nm/°C, which had been reported in our previous work, and the filtering efficiency (slope of falling curve) can be maintained when the cutoff wavelength is tuning far away from the origin [11]. Based on the same principle, a local liquid-core single-mode fiber was used to achieve widely tunable long-pass filters [12] and finally a bandpass filter

* Corresponding author.

E-mail address: jessica.eo91g@nctu.edu.tw (K.-C. Hsu).

with a wide tuning bandwidth can be made by concatenating one short-pass and one long-pass filters. The spectral envelope of the bandpass filter can be further engineered to fit the Gaussian profile based on the modification of the waveguide dispersion determined by the fiber diameter and the modification of the interaction length. Consequently, based on the material and waveguide dispersion engineering, we, for the first time, propose a widely tunable broadband all-fiber Gaussian-shaped spectral filter by concatenating a SWPF and a LWPF. Preliminary experimental and theoretical results show that the generated Gaussian-spectral lights can have a spectral contrast ratio higher than 40 dB, which should be useful for the OCT bio-imaging applications.

2. Simulation and experiment

To achieve spectral Gaussian filters operating over 1250–1650 nm, a LWPF with a rising Gaussian-shaped cut-on curve at the shorter wavelength side and a SWPF with a falling Gaussian-shaped cutoff curve at the longer wavelength side are discretely employed. The RID curves for the various Cargille liquids (Cargille index-matching liquid with the index $n_D = 1.456$ and the thermo-optic coefficient $dn_D/dT = -3.74 \times 10^{-4}/^\circ\text{C}$) and the fused silica glass are shown in Fig. 1(a). The liquids have a flatter RID slope than fused silica due to their lower phonon energies [12]. In Fig. 1(a), the cross point of the RID curves of the silica and optical liquid ($n_D = 1.456$) are labeled by P . From the two RID curves, in the left-hand side of P point SWPFs can be achieved when the fused silica and optical liquid respectively plays as the core and cladding [11]. Light guiding is only satisfied for the wavelengths shorter than the P point but frustrated at other side of P point and thus great amounts of optical losses are introduced there. On the contrary, in the right-hand side of P point LWPFs can be realized when the roles played by the fused silica and optical liquid are reversed [12]. The cross angle θ between the two RID curves decides the filtering efficiency and a larger θ can more clearly discriminate the passband and stopband wavelengths and gives rise to a sharper rising or falling curve for the filters. A very sharp rising or falling curve is crucial for the fiber-optic communication systems to clearly separate the desired and unwanted signals but may not be suitable for the low coherence tomography imaging systems in which a broadband Gaussian light source is required to obtain high quality images. A broadband Gaussian spectrum naturally comes along with slowly varying rising and falling spectral curves and therefore the spectral envelope of the bandpass filter must be further adjusted. The adjustments of the slope for rising and falling curves of filters can not only be done by engineering the material dispersion, namely the use of suitable liquids, but also by engineering the waveguide dispersion, namely the modification of the fiber structure. We can reshape the rising and falling curves to fit the Gaussian profile by selecting suitable diameter of tapered waist D , length of tapered waist L_W , and length of tapered transition L_T . In this work the cutoff and cut-on curves of the SWPFs and LWPFs are numerically simulated by adopting the beam propagation method (BPM) to determine the optimal waveguide structures for an ideal Gaussian-shaped spectrum and some experimental results are demonstrated to show the thermo-optic tuning ability. Further optimized can be taken in the future to attain better Gaussian-shaped spectral filtering function.

Numerical simulation using the beam propagation method (BPM) is performed to theoretically analyze the fundamental-mode cutoff characteristics and study the optical field propagation within the tapered region of the standard single-mode fibers. The fiber taper transition structure is set to be an exponential shape, and a fundamental fiber mode is launched into the transition region to estimate the mode coupling and mode conversion effects along the fiber taper with dispersive liquids surrounded. The fun-

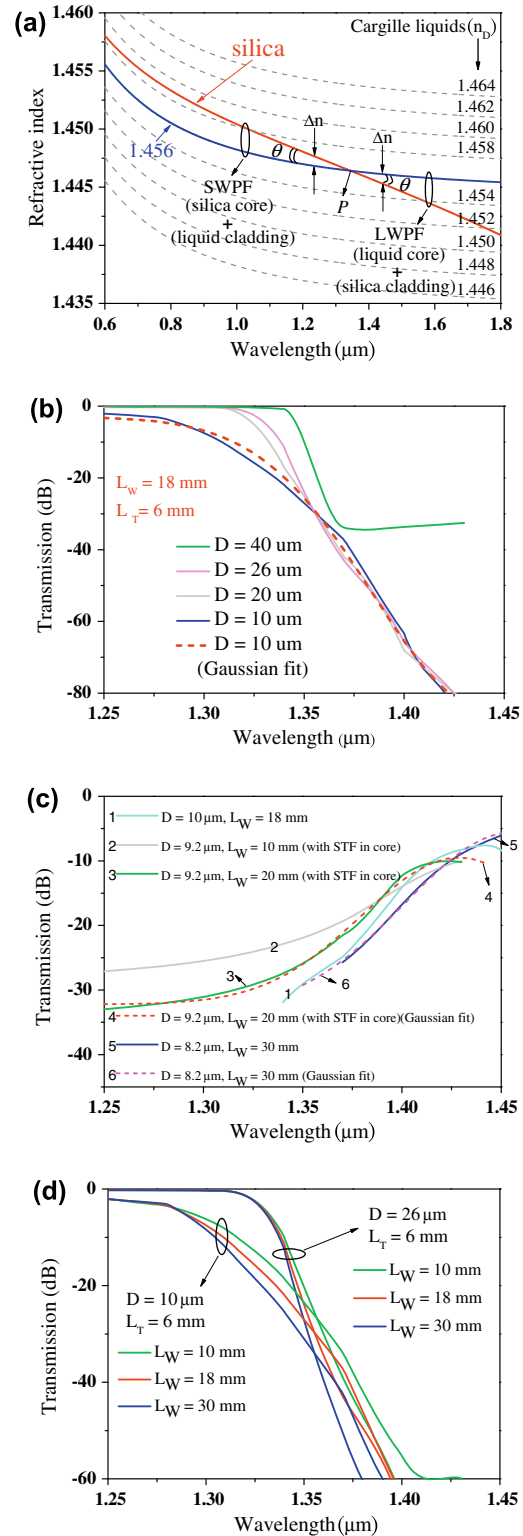


Fig. 1. (a) Refractive index dispersion of silica and Cargille optical liquids. (b) Simulated transmission spectra of the SWPFs at different diameters of tapered waist and the Gaussian fit curve. (c) Simulated transmission spectra of the LWPFs at different diameters of liquid-core and the Gaussian fit curves. (d) Simulated transmission spectra of the SWPFs at different lengths of tapered waist.

damental eigenmode of the input SMF fiber is smoothly transformed into the fundamental eigenmode of the uniform taper waist, and the field propagates through the uniform waist region and then gradually re-converts to the fundamental mode of the output SMF within the second transition zone. The fundamental

modes corresponding to wavelengths with 10-nm separation are sequentially launched into the tapered fiber, and the output optical powers normalized to the input powers are estimated as transmission loss. BPM simulations with different taper parameters for SWPFs and LWPFs are respectively performed for determining the optimal taper structures to yield the half part of the spectral Gaussian shape. The simulated transmission spectra of the SWPF and LWPF are respectively shown in Fig. 1(b) and (c) with the key parameters indicated. In Fig. 1(b), when D gradually goes down toward $10\ \mu\text{m}$, the slopes of the falling curves get flatter since the waveguide dispersion only dominates the net dispersion at smaller D . Thus a smaller D can make the shorter wavelengths more lossy. The curve of $D = 10\ \mu\text{m}$ can fit the Gaussian profile quite well and the attenuation can be as high as 80 dB. When this Gaussian fit falling curve combined with its mirror image to form a complete Gaussian profile, a broadband Gaussian signal with strong spectral contrast can be generated.

For the LWPFs, the fabrication method is by stretching a borosilicate capillary with a threaded submicron tapered fiber (STF) inside, until the inner diameter of the capillary decreases to a few micrometers. The stretched capillary with an STF inside is then infiltrated with optical liquids to act as a new core, and LWPFs can thus be achieved. The mode fields of the guiding lights are strongly extended to the outside of STF and tightly overlapped with optical liquids. The dispersion of the guiding lights can be strongly changed by the local liquid-core/borosilicate-cladding structure [12]. In Fig. 1(c), a submicron tapered fiber (STF) with a liquid-core diameter D of 950 nm [12] is also simulated to engineer the dispersion for the best Gaussian fit. The slope of the rising curve and the attenuation for LWPFs are flatter and smaller than that of SWPFs. This is because even when the LWPF and SWPF are using the same silica and optical liquid to produce the same θ and the same index difference Δn near P point in Fig. 1(a), the mode field distribution is larger at the longer wavelength side for the LWPFs and thus the poor confinement leads to a flatter cut-on curve and smaller spectral contrast. However, a longer L_w can be utilized to achieve a shaper cut-on curve for Gaussian fitting and, from Fig. 1(c), the rising curves of the LWPFs can also fit the desired Gaussian profiles. Simulated transmission spectra of the SWPFs at different length of tapered fibers are also shown in Fig. 1(d). The adjustment of L_w can also help to fit the Gaussian profile for the cases of smaller D .

The spectral Gaussian filter can be achieved by combining a rising-Gaussian cut-on curve from the SWPF and a falling-Gaussian cutoff curve from the LWPF. To generate the falling-Gaussian cutoff curve, Fig. 2(a) shows the waveguide structure of the SWPF. It consists of a transmission zone, where the fiber diameter gradually reduced over the distance, and a uniform-waist section in the middle. The fused-tapered fiber is immersed with index-matching liquids, and the optimal D is around $10\ \mu\text{m}$ by simulation, seen from Fig. 1(b). The total elongation length is about 30 mm, and the length of the uniform waist is measured to be around 18 mm. The tapered fiber filter fabricated by our homemade tapering workstation which integrates several parts including the pulling mechanism, heating system, scanning mechanism, and real-time monitor system, as has been shown in Fig. 2(b). A hydrogen flame with stabilized flow control set on a three-axis stepper motor forms the main part of the heating system and scanning mechanism. This setup allows precise positioning of the flame and the flame is allowed to scan over a large heating-zone. When the tapering process begins, the pulling motors move outward to elongate the fiber and the flame starts simultaneous zigzag scanning to enlarge the effective heating-zone. This process ensures that the flame heats identically each section of the fiber being tapered in each cycle of scanning. As long as the heating-zone can be controlled precisely, the length of the uniform waist of the tapered fi-

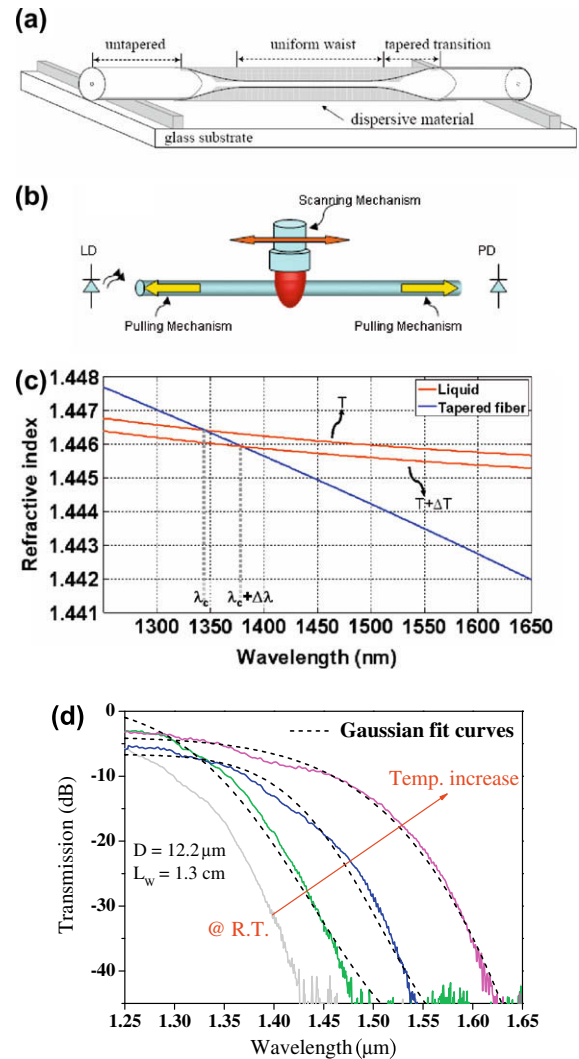


Fig. 2. (a) Diagram of a tapered optical fiber (SWPF) with a uniform waist. (b) Schematic diagram of the tapering station used to fabricate the tapered fibers. (c) Refractive index dispersion curves with different temperature. The solid line depicts the tapered fiber, and the dotted line indicates the index-matching liquid with different temperatures. (d) Spectral responses and fitted Gaussian curves of SWPF at different temperatures.

ber is controllable. The pulling mechanism has two high-precision stepper motors with simultaneous start/stop design and drives two V-groove holders that can mount a single-mode fiber and provide a constant stress. One end of the single-mode fiber is connected to superluminescent diodes (LD) and the other end is connected to a photo-detector (PD) to form a real-time monitoring system, which can help determine the best stop-point for the stretching procedure. When finishing tapering, the fiber is fixed in a U-groove on a quartz substrate and then immersed in index-matching liquid. A TE-cooler is used to control the liquid temperature to change its refractive index and the cutoff wavelength turns out to be tunable. When a single-mode optical fiber is tapered to tens of micrometers in diameter, the evanescent waves spread out into the cladding and reach the external environment and the size of the core in the tapered zone is so reduced that its waveguiding effects are negligible. Therefore, the cladding plays the role of core and the external medium plays the role of cladding. Fig. 2(c) shows the refractive index dispersion curves of the index-matching liquid (red) and tapered fiber (blue) at different temperatures. At the right side of the cross point (λ_c), the refraction index of the liquid is greater than the index of fiber taper and the total internal reflection is frustrated.

Therefore the lights cannot be guided in the fiber taper and suffer great amount of optical losses. On the other hand, the light can be confined in fiber taper when the wavelength is located at the left-hand side of the cross point. The cutoff wavelength of a short-wavelength-pass filter approximately locates at the cross point. As the temperature increases, the refractive index of the surrounding liquid decreases. Heating up the liquid causes the dispersion curve shift downward and the cross point will move to longer wavelengths. By heating up or cooling down the liquid (temperature changes from T to $T + \Delta T$), we can continuously tune the band-edge wavelength, as shown in Fig. 2(c). The gray line in Fig. 2(d) is the initial cutoff curve of the tapered fiber immersed in optical liquid at room temperature (RT) and the liquid is then heated up by a 175 W infrared lamp which is located 20 cm away from the tapered fiber. When the liquid is respectively heated up by the infrared lamp with an increment of 5 s for each run time, three different falling curves are obtained as shown in Fig. 2(d), with their slopes getting flatter and flatter. The P point of the SWPF moves to longer wavelengths with increasing temperature so that the passband bandwidth becomes wider. The achieved spectral contrast is higher than 40 dB for all curves, which is advantageous for practical applications. The cutoff curves become slowly falling down since the waveguide dispersion significantly dominates the dispersion when D decreases to be less than 10 μm . The optical field strongly spread out into the optical liquid and becomes less dispersive. The falling curves are individually Gaussian-fitted and the Gaussian fit curves are also displayed as dotted lines shown in Fig. 2(d), where in particular the experimental data of the pink line can fit the Gaussian profile and the simulation results excellently well. In principle, the long-pass filter based on liquid-core fiber [12] can also produce Gaussian-shaped curves as predicted in Fig. 1(c). Consequently, the concatenated Gaussian-shaped band-pass filter will be widely tunable ascribing to the high thermo-optic coefficient of optical liquids [12]. The wideband tunable Gaussian-shaped spectral filter can be further optimized by carefully considering both material dispersion and waveguide dispersion. The proposed spectral filter provides a potential technique in application to high resolution bio-imaging.

3. Conclusions and summary

We have proposed a new method of achieving widely tunable all-fiber broadband Gaussian-shaped spectral filters by concate-

nating thermo-optic tunable short-pass and long-pass filters. The material and waveguide dispersions are both employed to vary the spectral envelope of SWPFs and LWPFS to respectively fit the right and left wings of the desired Gaussian profile. The achieved spectral contrast can be higher than 40 dB and the filter still keeps Gaussian-shaped during thermo-tuning process. This kind of widely tunable Gaussian filters should be advantageous for OCT bio-imaging systems using broadband light sources.

Acknowledgments

This work was funded by grants from the Republic of China National Science Council (NSC 97-2218-E-239-003 & NSC 96-2221-E-155-039-MY3 & 97-2923-E-011-001-MY).

References

- [1] A. Unterhuber, B. Povazay, K. Bizheva, B. Hermann, H. Sattmann, A. Stingl, T. Le, M. Seefeld, R. Menzel, M. Preusser, H. Budka, Ch. Schubert, H. Reitsamer, P.K. Ahnel, J.E. Morgan, A. Cowey, W. Drexler, Advances in broad bandwidth light sources for ultrahigh resolution optical coherence tomography, *Phys. Med. Biol.* 49 (2004) 1235.
- [2] S.K. Dubey, D.S. Mehta, A. Anand, C. Shakher, Simultaneous topography and tomography of latent fingerprints using full-field swept-source optical coherence tomography, *J. Opt. A: Pure Appl. Opt.* 10 (2008) 015307.
- [3] K. Grieve, G. Moneron, A. Dubois, J. Gargasson, C. Boccard, Ultrahigh resolution ex vivo ocular imaging using ultrashort acquisition time en face optical coherence tomography, *J. Opt. A: Pure Appl. Opt.* 7 (2005) 368.
- [4] H.S. Djie, C.E. Dimas, D.N. Wang, B.S. Ooi, J.C.M. Hwang, G.T. Dang, W.H. Chang, InGaAs/GaAs quantum-dot superluminescent diode for optical sensor and imaging, *IEEE Sens. J.* 7 (2007) 251.
- [5] B.E. Bouma, G.J. Tearney, Handbook of Optical Coherence Tomography, Marcel Dekker, New York, 2002 (Chapters 2, 3, and 7).
- [6] G. Contestabile, R. Proietti, N. Calabretta, M. Presi, A. D'Errico, E. Ciaramella, Simultaneous demodulation and clock-recovery of 40-Gb/s NRZ-DPSK signals using a multiwavelength Gaussian filter, *IEEE Photon. Technol. Lett.* 20 (2008) 791.
- [7] A. Chong, W.H. Renninger, F.W. Wise, Environmentally stable all-normal-dispersion femtosecond fiber laser, *Opt. Lett.* 33 (2008) 1071.
- [8] A. D'Errico, WDM-DPSK detection by means of frequency-periodic Gaussian filtering, *Electron. Lett.* 42 (2006) 112.
- [9] I.C.M. Littler, M. Rochette, B.J. Eggleton, Adjustable bandwidth dispersionless bandpass FBG optical filter, *Opt. Express* 13 (2005) 3397.
- [10] L. Scolari, T.T. Alkeskjold, A. Bjarklev, Gaussian filtering with tapered liquid crystal photonic bandgap fibers, in: Proc. of LEOS 2006 ThN3, 2006.
- [11] N.K. Chen, K.C. Hsu, S. Chi, Y. Lai, Tunable Er^{3+} -doped fiber amplifiers covering S and C+L bands over 1490–1610 nm based on discrete fundamental-mode cutoff filters, *Opt. Lett.* 31 (2006) 2842.
- [12] N.K. Chen, S. Chi, Novel local liquid-core single-mode fiber for dispersion engineering using submicron tapered fiber, in: Proc. of OFC 2007 JThA5, 2007.